Dynamic Behavior of Hydraulic Wash Columns

L. van Oord-Knol
DSM Research, Centre for Particle Technology, 6160 MD Geleen, The Netherlands

O. S. L. Bruinsma
Sasol Center for Separation Technology, Potchefstroom University for CHE, Potchefstroom 2520, South Africa

P. J. Jansens
Laboratory for Process Equipment, Delft University of Technology, Leeghwaterstraat 44, 2628 CA Delft, The Netherlands

Hydraulic wash columns are well suited for solid–liquid separation and ultrapurification in melt-suspension crystallization. For steady operation of a hydraulic wash column and proper purification, the length of the crystal bed and position of the wash front should stay within safe limits, which requires a well-defined control system. To understand the interactions between slurry properties, column dimensions, and process conditions, a dynamic model was developed. The model was validated with help of experiments in a pilot-plant wash column, fed from a continuous crystallizer. P-Xylene was used as the model compound. It satisfactorily predicted the trends in the length of the crystal bed and the wash front height, and the interactions in the wash column are largely understood. With the help of the model a feedback control system with two control loops was designed and simulated. For a wide range of crystal fractions (0.05 to 0.3 v/v) in the feed stream, both the length of the bed and the wash front were kept at the desired setpoint values, indicating the flexibility of a controlled wash column.

Introduction

Melt crystallization processes facilitate the ultrapurification of organic compounds at relatively low energy consumption compared to distillation processes, while the use of solvents like in extraction processes is avoided. To reach the desired purity solid–liquid separation and washing can be performed in so-called wash columns. Three types of wash columns can be distinguished, according to the transport mechanism of the solids: gravitational, mechanical, and hydraulic. Industrial designs are mentioned for all three types in the literature. In hydraulic wash columns transportation of the packed bed is due to the liquid pressure drop over the bed (Arkenbout, 1995).

The working mechanism of the TNO-Thijssen-type hydraulic wash column is illustrated in Figure 1. A more detailed description of the column can be found in van Oord-Knol et al. (2002). A feed slurry is pumped into the top of the wash column. Due to the drag of the mother liquor, the crystals are transported through a short slurry zone to reach a packed bed of crystals. The mother liquor flows through the packed bed to leave the column via filters positioned in filter tubes, thus creating the force to transport the crystals through the column. A steering pump can be used to recycle the mother liquor into the top of the wash column to alter the transport force at constant feed conditions. At the bottom of the wash column the crystals are scraped off by a rotating knife and fall into the melt, which is circulated through the reslurry chamber and the melting circuit, where all crystals are molten. The major part of the pure melt, the product, leaves the melting circuit via the product valve.

The product valve is used to create a small excess pressure in the reslurry chamber, so that the residual part of the melt is forced back into the column to perform a countercurrent washing action. The pure wash liquid is at melt temperature and crystallizes on the downward-moving crystals, which are still at feed temperature. In this way the wash liquid solidifies before it is lost via the filter tubes and forms a sharp wash front, which marks a sharp decrease in porosity and permeability. When hydraulic wash columns are used in nonmelt applications, the wash liquid will not solidify on the crystals

Correspondence concerning this article should be addressed to L. V. Oord-Knol.

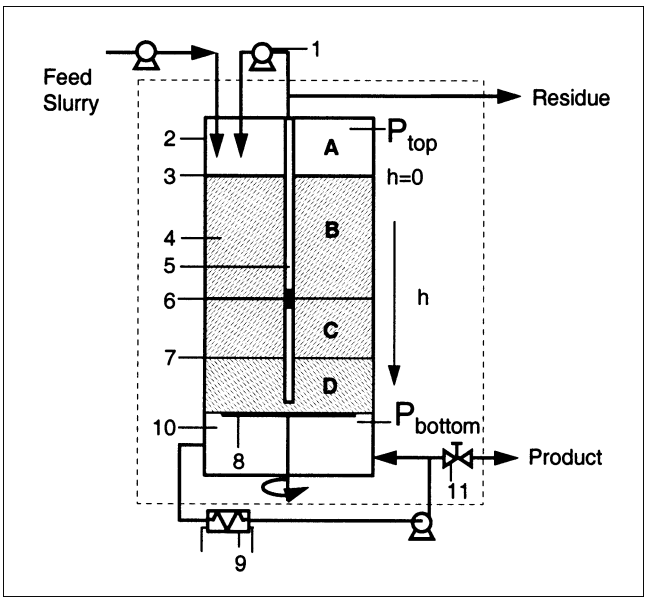

Figure 1. Principle of a hydraulic wash column.

1 = Steering pump; 2 = column wall; 3 = bed level; 4 = moving packed bed; 5 = filter tube; 6 = filter; 7 = wash front level; 8 = rotating knife; 9 = melter; 10 = reslurry chamber; 11 = product valve. A = slurry section; B = filtration section; C = stagnant section; D = wash section.

and is therefore lost via the filters. Since this is the main difference in wash-column operation, theories developed for wash columns in melt crystallization can be applied to solution crystallization as well.

For a steady operation and purification, the length of the crystal bed and the position of the wash front should stay within safe limits. The bed height must not be too high to prevent filling of the slurry section, while, on the other hand, a minimum bed height is needed to guarantee a transport force that is large enough to counteract the liquid pressure in the bottom section and the wall friction. The optimal position of the wash front is below the filters to prevent loss of wash liquid and the blocking of the filter tubes by wash-liquid crystallization. For ultrapure products the wash-front level should be kept well above the knife, so that no mother liquor can leak into the melting circuit.

Although the hydraulic wash column was successfully used for the solid–liquid separation and purification of several organic compounds from multicomponent mixtures on a pilot scale (Nienoord et al., 1994), there still are no references to hydraulic wash columns working on an industrial scale. More insight in scale-up rules and in the influence of slurry properties on the wash-column performance might enhance their introduction in industry. Therefore, the way in which the column is optimally operated and controlled has to be examined on a pilot scale and with the help of wash-column models. A general control strategy based on empirical observations was developed by Jansens et al. (1994a). They describe how the steering flow and the product valve can be used as control tools for the level of the bed and the wash front. However, no quantitative predictions of the effect of a control action on the length of the bed, the position of the wash front, and the expected liquid pressure were reported. In addition, the influence of the slurry properties and column dimensions on the dynamic behavior were not investigated.

The objective of this study is the derivation of a dynamic hydraulic wash-column model that takes into account both slurry properties and column dimensions. The developed model is validated in a pilot plant containing a TNO-Thijssen-type wash column connected to a continuous suspension crystallizer, with a xylene mixture as the model compound. Finally, controllers are implemented in the model to investigate the effect of control actions.

Model Formulation

Definition of the system

Figure 1 is a drawing of the hydraulic wash column, where the chosen system boundary is shown by the dotted line. With this system boundary the inputs are the feed flow, the temperature and the crystal concentration in the feed, the steering flow, and the opening of the product valve. The output variables of the model are the total bed height and the position of the wash front, which should be controlled for proper operation. Additional outputs are the residue flow, the product flow, and the pressure at the top of the bed, P_{top}, and in the melting circuit, P_{bottom}.

To derive the model three main sections are defined: the top section, the bottom section, and the melting circuit. The top section stretches from the top of the wash column to the filters. It consists of the slurry section (A), where a loose slurry is present, and the filtration section (B), which is the part of the packed bed between the top of the bed and the filters. Since the position of the filters is fixed, the position of the crystal bed is determined by the length of the filtration section, $L_{filtration}$ (m).

The bottom section stretches from the filters to the knife and is totally occupied by the packed bed. The bottom section is subdivided into the stagnant zone (C) and the wash section (D). The packed bed pores in the stagnant zone are filled with mother liquor, while the pores in the wash section are filled with wash liquid. The position of the wash front therefore corresponds to the length of the wash section.

The melting circuit consists of several parts: the reslurry chamber (10), the circulation pump, the smelter, and all tubing between these pieces of equipment and the product valve.

Assumptions

The dynamic model is based on the assumption that the column is totally filled with liquid and crystals, which are both incompressible. A consequence of this assumption is that in the model derivation volume is the conserved unit instead of mass. In addition, for the sake of simplicity, it is assumed that the density and the viscosity of the wash liquid are equal to the density and viscosity of the mother liquor and are both temperature independent.

To calculate the pressure drop in the three sections of the wash column, one-dimensional flow is assumed. This assumption is justified for large aspect ratios and a relatively large surface area of the filters compared to the cross-sectional area of the column. The aspect ratio, defined as the ratio between the distance the liquid has to move in the axial and radial direction, ranges from 10 to 25 for the used wash column,

depending on the length of the packed bed. This is large enough to justify this assumption.

It is assumed that due to wash-liquid crystallization there is an abrupt porosity and permeability change at the wash front. It is further assumed that the porosity and permeability in each of the defined sections are constant, which means that consolidation of the crystal bed is neglected. It was shown that consolidation in the filtration section influences the production capacity of the wash column, and this assumption therefore limits the applicability of the model to operation conditions with production rates that are on the same order of magnitude as those used in the validation experiments (van Oord-Knol, 2000). For considerably higher throughputs, the permeability and porosity, and, thus, the calculation of the pressure level, may differ from the predicted values. For these high production rates, it is advised that axial porosity and permeability profiles be incorporated.

The calculations are based on a column that is adiabatic above the knife, while in the melting circuit just enough heat is applied to melt all the crystals, so that the wash liquid that reenters the column is at the melt temperature. The wash liquid does not reach the filters, which is in general aimed for, since loss of wash liquid has to be prevented.

Finally, it is assumed that the crystal bed does not rest on the knife, either in the dynamic or in the steady state, which means that the stress on the knife is zero. This is true if the rotational speed of the knife does not limit the product flow rate, which is the preferred way of operating the hydraulic wash column.

Volume balances for the top section

In the top section there are two phases present, crystals and mother liquor.

An overall volume balance for the top section gives

$$\varphi_{\text{feed}} + \varphi_{\text{steer}} = \varphi_{s,\text{filters}} + \varphi_{ml,\text{filters}} \tag{1}$$

where $\varphi_{s,\text{filters}}$ (m^3/s) is the amount of solid material that leaves the top section to enter the bottom section at the filters, and $\varphi_{ml,\text{filters}}$ (m^3/s) is the mother liquor flow from the top section that leaves the column via the filters.

The length of the filtration section is calculated with help of the solids balance in the top section

$$\frac{dV_{cr,\text{top}}}{dt} = \alpha_1 \cdot \varphi_{\text{feed}} - \varphi_{s\text{filters}} \tag{2}$$

The total amount of solid material in the top section is distributed over the slurry section and the filtration section

$$V_{cr,\text{top}} = A_c \cdot \left[(1-\epsilon) \cdot L_{\text{filtration}} + \alpha_2 \cdot L_{\text{slurry}} \right] \tag{3}$$

The required parameters are the porosity of the crystal bed, ϵ, and the concentration of the crystals in the slurry section, α_2. It is assumed that the crystal concentration in the slurry section equals the crystal concentration in the stream, which enters the wash column after mixing the crystal-free steering flow with the feed flow, having crystal concentration α_1. Since the total length of the top section is constant, the length of the filtration section is calculated by combining Eqs. 2 and 3

$$\frac{dL_{\text{filtration}}}{dt} = \frac{1}{A_c \cdot (1-\alpha_2-\epsilon)} \cdot (\alpha_1 \cdot \varphi_{\text{feed}} - \varphi_{s,\text{filters}}) \tag{4}$$

Bottom section: Overall balance and two liquid balances

In the bottom section one solid phase, the crystals, and two liquid phases, wash liquid and mother liquor, are present. The total volume of the bottom section is constant; therefore, an overall volume balance for the bottom section combines the flows entering and leaving with the volume of the solid material that is created by crystallization (C_s) and the volume of the wash liquid that disappears (C_l) due to the same crystallization

$$\varphi_{s,\text{filters}} + C_s + \varphi_{wl,\text{knife}} = \varphi_{ml,\text{bottom}} + \varphi_{s,\text{knife}} + C_l \tag{5}$$

Due to the density difference between solid and liquid material, the volumes C_s and C_l are not equal. Since these volumes represent the same mass, the solid and the liquid densities are used to relate those volumes

$$C_l = \frac{\rho_s}{\rho_l} \cdot C_s \tag{6}$$

It is assumed that the total cooling capacity of the descending crystals is used to crystallize the ascending wash liquid. The amount of crystallized material can be calculated from a heat balance and the temperature difference between the feed slurry and the melt

$$C_s = \frac{c_P \cdot (T_{\text{melt}} - T_{\text{feed}})}{\Delta H_m} \cdot \varphi_{s,\text{filters}} \tag{7}$$

The volume of wash liquid in the wash column changes due to the wash-liquid flow entering at the knife, said to be positive, and by the wash liquid that crystallizes. It is assumed that the wash front does not reach the filters and therefore, there is no loss of wash liquid out of the column via the filters. The length of the wash section is directly related to the wash liquid volume; therefore

$$\epsilon_w \cdot A_c \cdot \frac{dL_{\text{wash}}}{dt} = \varphi_{wl,\text{knife}} - C_l \tag{8}$$

The porosity in the wash section is calculated from a simple heat balance and the porosity in the top section

$$\epsilon_w = \epsilon - (1-\epsilon) \cdot \frac{c_P \cdot (T_{\text{melt}} - T_{\text{feed}})}{\Delta H_m} \tag{9}$$

When the length of the wash section changes, mother liquor will flow into or out of the bottom section. Defining a mother-liquor flow out of the section positive gives

$$A_c \cdot \epsilon \cdot \frac{dL_{\text{wash}}}{dt} = \varphi_{ml,\text{bottom}} \tag{10}$$

Both the mother liquor from the top section and the bottom sections leave the column via the filter tubes to split again into the steering flow and the residue flow. So the residue flow, which is an output variable, can be calculated as follows

$$\varphi_{\text{residue}} = \varphi_{ml,\text{bottom}} + \varphi_{ml,\text{filters}} - \varphi_{\text{steer}} \tag{11}$$

Melting circuit

The crystals from the packed bed leave the bottom section via the knife. All crystals have to be molten, as the product is a liquid. Assuming that the crystals are molten at the moment they enter the melting circuit, the following mass balance holds, where a correction is needed for the density difference between solid and liquid

$$\frac{\rho_s}{\rho_l}\cdot\varphi_{s,\text{knife}} = \varphi_{wl,\text{knife}} + \varphi_{\text{product}} \tag{12}$$

All volume balances are defined with Eq. 12. The equations that in fact form the skeleton of the model are Eqs. 1, 4, 5, 8, 10, 11 and 12. The other equations are additional equations that contain the necessary parameters. To calculate the remaining output variables, that is, P_{top} and P_{bottom}, a force balance which will be described in the following section, is needed.

Force balance

Figure 2 shows the stress distribution in the packed bed, which is caused by the forces working on the bed: the drag forces due to the liquid flow through the bed, the friction with the wall and the filter tubes in the column, and the gravity and buoyancy forces. These last two forces are neglected in the model, as for organic compounds these forces are two orders of magnitude smaller than the force usually created by the liquid pressure drop.

Assuming liquid flow in axial direction only, a force balance over a horizontal slice of the crystal bed in the column (Figure 2) results in the following equation

$$\frac{d\sigma(h)}{dh} = -\frac{dp_l(h)}{dh} - \frac{4}{D}\tau_w(h) \tag{13}$$

According to the theory of Janssen (1895) the shear stress at the wall, τ_w (Pa), can be calculated from the radial compressive stress, σ_r (Pa), and the wall friction coefficient, μ_w, and the ratio between radial and axial stress, K, as follows

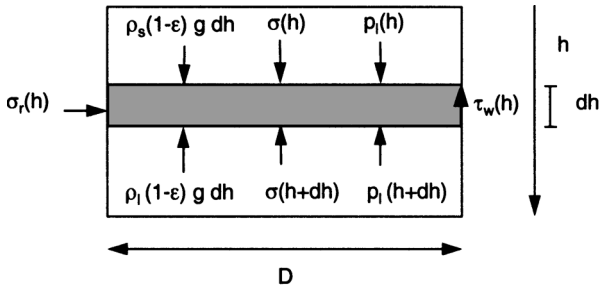

Figure 2. Stress distribution on a slice in the packed bed.

$$\tau_w(h) = \sigma_r(h)\cdot\mu_w = \sigma(h)\cdot\mu_w\cdot K = K_f\cdot\sigma(h) \tag{14}$$

The wall friction coefficient and the stress ratio K are often combined to give the friction factor, K_f. Several authors have presented methods to determine the friction factor, K_f, in the wash column (Schneiders and Arkenbout, 1986; Jansens et al., 1994b; van Oord-Knol, 2000). Since the porosity of the packed bed decreases in the top section and the crystal shape and morphology change due to melting and freezing phenomena at the wash front, it is likely that the friction factor will change in the packed bed. However, no method has been developed to measure these local friction factors. In the model it is therefore assumed that the friction factors for the column wall and the filter tubes are equal and constant for the total length of the packed bed.

The compressive stress profile in the wash column can be calculated from the liquid pressure drop in each section of the packed bed, combined with the friction factor and with the compressive stress at the top of the crystal bed. At the top the stress is zero, as there has been no drag force on the particle bed. When the cutting capacity of the knife is larger than the solids flow, the bed does not rest on the knife and there is no restraining force from the knife. So that the compressive stress at the knife is zero

$$\sigma_{\text{knife}} = 0 \tag{14a}$$

In the Appendix the equations for calculating the compressive stress and the liquid pressure drop in each section are given, with which Eq. 14 can be solved. The liquid pressure drop over a section of the packed bed can be calculated with a modified Darcy equation (Shirato et al., 1969) to take the solids velocity into account. For the filtration section, this gives

$$\frac{\Delta P_{l,\text{filtration}}}{L_{\text{filtration}}} = \frac{-\epsilon\cdot\eta_l}{B_{\text{filtration}}}\cdot\left(\frac{\varphi_{ml,\text{filters}}}{\epsilon\cdot A_c} - \frac{\varphi_{s,\text{filters}}}{(1-\epsilon)\cdot A_c}\right) \tag{15}$$

Since the bed is assumed to be incompressible, the porosity and the permeability in a section are constant, and, thus, the liquid pressure gradient is constant. The liquid pressure profiles in each section are also used to calculate the pressure at the top and at the bottom of the column. The liquid pressure at the top, that is, the pressure in the slurry section, is calculated from the pressure at the filters and the pressure drop over the filtration section, caused by the mother liquor flow through the packed bed

$$P_{\text{top}} = P_{\text{filters}} + \Delta P_{l,\text{filtration}} \tag{16}$$

The liquid pressure at the bottom of the packed bed equals the pressure in the melting circuit. The valve in the melting circuit relates the product flow to the pressure in the melting circuit. The pressure drop over the valve depends on the type of valve, the size of the valve, and the product flow rate

$$\Delta P_{l,\text{valve}} = f(\varphi_{\text{product}}) \tag{17}$$

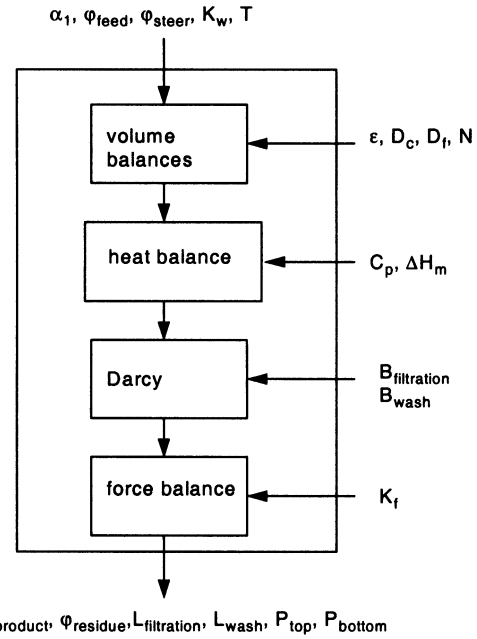

Figure 3. Dynamic model with its inputs, outputs, and parameters.

In the model, a linear relation between the product flow and the pressure in the melting circuit was used

$$\Delta P_{l,\text{valve}} = K_w \cdot \varphi_{\text{product}} \tag{18}$$

The pressure after the valve is said to be atmospheric, and, therefore, the pressure drop over the valve equals the pressure in the melting circuit. The pressure in the melting circuit is related to the pressure at the filters and the pressure drop in the stagnant and wash sections as follows

$$P_{\text{bottom}} = \Delta P_{l,\text{valve}} = \Delta P_{l,\text{stagnant}} + \Delta P_{l,\text{wash}} + P_{\text{filters}} \tag{19}$$

The pressure drops over the stagnant zone and the wash section are calculated with the appropriate values for the local porosity and permeability and the liquid flow, as shown in the Appendix.

With the force balance the dynamic model for the hydraulic wash column is completed. Figure 3 summarizes the model with the input variables, output variables, and the required parameters. It shows that all the important outputs can be calculated:

- The length of the bed and the position of the wash front, which are important for proper operation of the wash column.
- The output flows, which are the residue flow and the desired production; these should be known because of the effect on downstream operations.
- The pressure levels are important during operation, as they should not exceed the design values of the equipment and may influence pumps, as will be shown in the next section.

Table 1. Column Dimensions

Column diameter (m)	0.156
Length (m)	1
Number of filter tubes	6
Distance between filters and knife (m)	0.28
Filter length (m)	0.03
Filter tube diameter (m)	0.02

Experimental Procedure

Two series of experiments were performed in a 0.156-m-diam hydraulic wash column (TNO-Thijsen-type), containing six filter tubes and with dimensions as given in Table 1. For the first series this wash column is directly fed from a 70-L scraped surface crystallizer, and both the product flow and the residue flow are returned to the crystallizer. This setup results in the direct coupling of the wash column and crystallizer dynamics, which appeared to complicate the validation of the model of the wash column, as will be shown in the following sections.

To reduce the coupling, a 700-L insulated storage vessel was incorporated into the pilot plant for the second series. The conditions in the vessel are kept constant by circulating the slurry over the 70-L scraped surface crystallizer, where the mixture is cooled. Figure 4 shows the flow sheet of this new setup. The temperature in the vessel was continuously measured and displayed. The wash column is fed from the storage tank, and the product and residue flow leaving the wash column are returned to the storage vessel. The crystal slurry was produced from a xylene mixture that consisted of para-xylene and 11% (w/w) of its isomer ortho-xylene.

The residue, product, and steering flow were measured with positive displacement meters and recorded with a PC. The pressure in the feed inlet, the filtrate outlet and in the melting circuit were recorded as well. The position of the wash front was visualized by adding a small amount of red dye to the xylene mixture and was recorded manually, together with the length of the crystal bed. The process conditions varied, as given in Table 2.

Validation of the Dynamic Model

Additional relations

To validate the dynamic model, the dynamic response to a step change in the steering flow (st) or the product valve (va) was recorded for two different pilot-plant setups. The dy-

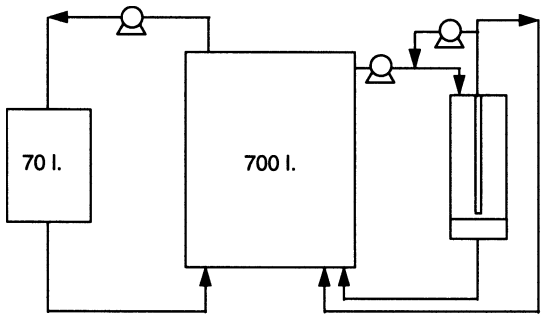

Figure 4. Pilot plant with storage vessel (setup II).

Table 2. Range of Process Conditions Used

Input variables		
Feed flow	400–850	L/h
Crystal concentration	0.08–0.12	v/v
Steering flow	0–890	L/h
Control valve opening	30–90%	
Output variables		
Length bed	33–92	cm
Length wash section	2–24	cm
Product flow	45–110	L/h
Residue flow	400–750	L/h
Pressure top	800–1800	mbar
Pressure bottom	500–900	mbar
Pressure filter	300–600	mbar

namic model presented in the previous section assumes a constant feed flow rate to the wash column, which is the preferred situation to prevent fluctuations in the conditions in the crystallizer. However, the feed pump in the used pilot plant appeared to be pressure dependent and a linear relation to describe the pump characteristic was included.

Another parameter that is said to be constant in the original model is the pressure at the filters, as it is assumed that the change in residue flow will not affect this value. In the experiments this was proven not to be correct, as is shown in Figure 5, where the pressure at the filters fluctuates between 400 and 600 mbar when the residue flow through the tubes varies from 550 to 700 L/h. Therefore, the pressure at the filters was made a linear function of the residue flow in the model, which seems to be justified by Figure 5b. The parameters that determine the filter-tube resistance had to be determined for every experiment, because longer tubing was used for the second setup.

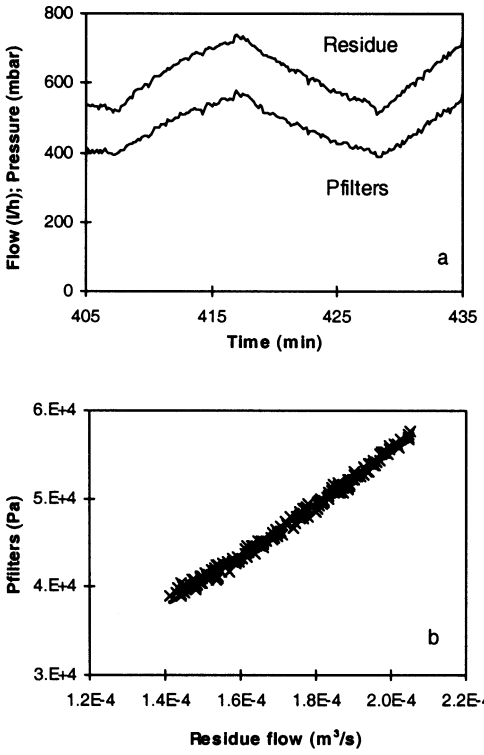

Figure 5. (a) Varying pressure at the filters with varying residue flow; (b) linear function to describe the relation between residue flow and pressure at the filters.

Table 3. Physical Properties P-Xylene

Viscosity (mPas)	0.683
Melting temperature (°C)	13.3
Heat capacity (KJ/kg·°C)	1.67
Heat of fusion (kJ/kg)	161.1
Solid density (kg.m^3)	1006
Liquid density (kg/m^3)	867

For model validation, simulations were carried out with the commercial code gPROMS (Barton and Pantelides, 1994). Several types of parameters are needed to perform these simulations. The physical properties of *p*-xylene are summarized in Table 3. For each experiment, the values of the input variables in the steady-state situation are summarized in Table 4. These are all controlled parameters: the steering flow can be adjusted via the steering pump, the crystal concentration of the feed stream can be changed by changing the crystallization conditions, and the resistance of the product valve is adjusted by closing or opening the valve. The steering flow is a measured variable, while the crystal concentration and valve resistance factor have to be derived from mass and force balances in the steady state. The characteristics of the crystal bed, the permeability of the top and bottom sections, and the friction factor were calculated from the steady-state measurements before the step change and are summarized in Table 5. The permeability was calculated from the measured liquid pressure drop, bed height and flow rates, and a constant porosity of 0.40 for the top section. The porosity in the bottom section follows from the heat balance and the porosity in the top section. The friction factor was fitted to equation (A7) in the Appendix, so that the compressive stress at the knife is zero for the process conditions valid in the steady-state situation. Both the permeability and the friction factor appeared to be lower in the setup without the storage tank. Different crystallization conditions clearly result in different crystal-size distributions, which will influence the behavior of the wash column.

Table 4. Input Variables for the Hydraulic Wash Column in Steady-State

Exp.	φ_{steer} (m^3/s)	α_1 (m^3/m^3)	K_w (Pa·s/m^3)
va-I	0	0.095	5.9×10^{9}
st-I	4.5×10^{-5}	0.082	5.9×10^{9}
va-II	1.6×10^{-4}	0.078	3.9×10^{9}
st-II	2.0×10^{-4}	0.12	2.7×10^{9}

Note: va: step change in position of the valve; st: step change in steering flow; I: setup without storage tank; II; setup with storage tank.

Table 5. Parameters Used in the Dynamic Simulations

Exp.	ϵ	$B_{filtration}$ (m^2)	B_{wash} (m^2)	K_f
va-I	0.40	0.890×10^{-11}	1.5×10^{-12}	0.068
st-I	0.40	0.93×10^{-11}	1.6×10^{-12}	0.084
va-II	0.40	3.4×10^{-11}	5.3×10^{-12}	0.13
st-II	0.40	4.3×10^{-11}	7.2×10^{-12}	0.11

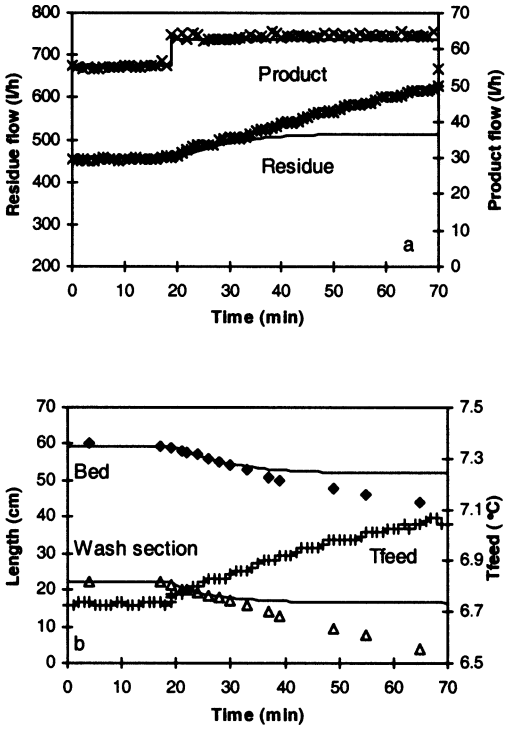

Figure 6. Simulated and measured dynamic response on opening the product valve.

K_w changes from 5.85×10^9 to 5.14×10^9 at $t=19$ min. (a) Product and residue flow; (b) length of bed and wash section, and temperature of feed slurry.

Validation in standard pilot plant: Product valve

In the standard pilot plant, with the crystallizer and wash column (setup I), the product valve resistance was decreased by opening the valve a little more at $t=19$ min. This was simulated by a decrease in valve resistance: K_w changed from 5.85×10^9 to 5.14×10^9. During the first 10 min after the step change, the experiment and simulation agree quite well, as shown in Figure 6. The product flow immediately increased from 55 L/h to 64 L/h, at a constant wash pressure. Both the length of the crystal bed and the wash section decreased.

However, Figure 6 also clearly shows how the simulated residue flow and the lengths of the crystal bed and wash section deviate from the measured values as time passes. This discrepancy is explained by the coupling between the wash column and the crystallizer. Because the product flow, which is the warm molten crystal stream, increases, the temperature in the crystallizer rises, and therefore, the temperature of the crystal slurry that is fed to the wash column, T_{feed}, rises about 0.35°C/h, as shown in Figure 6b. From the phase diagram of *p*-xylene, it can be calculated that the crystal fraction of the feed decreases from 0.095 to 0.054, for a change in temperature of 0.35°C, which means that fewer crystals enter the wash column, resulting in a lower bed level. This effectuates an increasing feed flow to the wash column, and thus an increasing residue flow. Furthermore, because of the higher residue flow, the residence time in the crystallizer decreases. In fact the feed slurry to the wash column will deviate more and more from the original feed slurry. This is valid both for the crystal concentration and crystal characteristics of the feed slurry. Unfortunately, no experimental data of the crystal concentration and permeability could be obtained during this experiment, since sampling would disturb the dynamic measurements too much.

Validation in standard pilot plant: Steering flow

The effect of the steering flow was also examined in setup 1. Figure 7 shows the simulated and measured dynamic response to a step change in a steering flow from 163 L/h to 35 L/h at $t=24$ min and back to 163 L/h at $t=35$ min. The length of the bed and the wash section are predicted quite well after the first step change. Note that the position of the wash front hardly changes on a step change in the steering flow. This contrasts with the effect of a change in the product valve, which influences both the bed level and the wash front level.

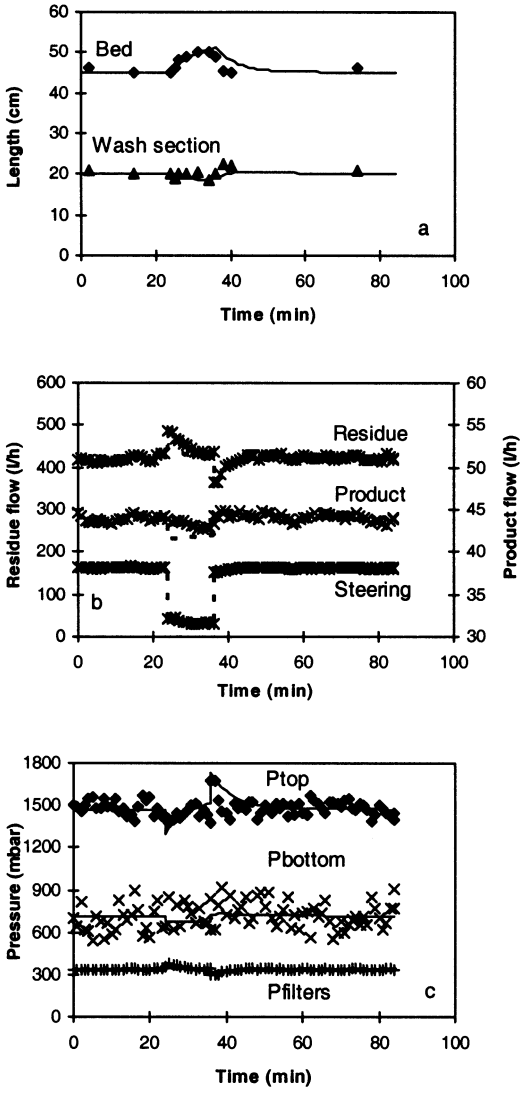

Figure 7. Dynamic response on a step change in the steering flow from 163 L/h to 35 L/h at $t=24$ min and back to 161 L/h at $t=36$ min.

(a) Length of the bed and the wash section; (b) flows; (c) pressures.

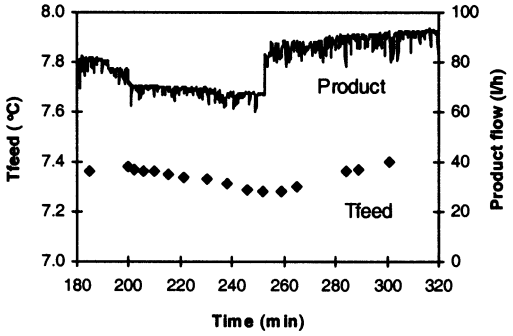

Figure 8. Temperature change after closing the product valve at $t = 200$ and opening at $t = 253$ with storage vessel.

Both the simulated and the measured residue flows increased at once, due to the sudden change in the top pressure and the reaction of the feed pump to this pressure change. The sudden change in the pressures is not so clear due to the scattering in the measured pressure; only the pressure at the filters shows the expected pressure jump.

Although in the first instance the simulations describe the phenomena in the wash column reasonably well, the fluctuations in the measured product flow and the measured pressures obscure proper assessment of the predicted steering-flow effect. In addition, validation of the effects of opening the valve were unclear due to the temperature changes. Therefore, a second series of experiments was carried out with a storage vessel between the crystallizer and the wash column.

Validation in the pilot plant with storage vessel: Control valve

The adjusted pilot plant (setup II) consists of a crystallizer, a storage vessel, and a wash column. Figure 8 shows that the temperature change, after a step change in the opening of the product valve, and, thus, in the product flow, is only 0.12°C/h when the product flow changes at 10 L/h, while for a step change of about 20 L/h the temperature changes only 0.18°C/h. Compared to the temperature change of 0.35°C/h in the standard pilot plant when the product flow changed about 10 L/h, the adjustment of the pilot plant is indeed an improvement.

In the adjusted setup, the control valve could be changed with larger steps, without disturbing the crystallizer too much. The values for K_w to simulate the applied steps in Figure 9 are given in Table 6.

Figure 9a shows that the product flow was changed with about 70 L/h in each step rather abruptly, while the residue flow, and thus the feed flow, slowly changed with time when the opening of the product valve was adjusted. The time between two step changes was about 10 min. This was the maximum time that could be chosen before the wash front reached the filters at 28 cm above the knife, or disappeared below the knife, as shown in Figure 9b. Both situations are undesirable, because the measured pressures and flows cannot be related to a representative length of the wash section anymore.

The effect on the length of the crystal bed and the wash section is shown in Figure 9b, while Figure 9c gives the simulated and measured pressures. The first impression is that the general trends in the simulations correspond quite well with the experiments. A closer look reveals some critical details.

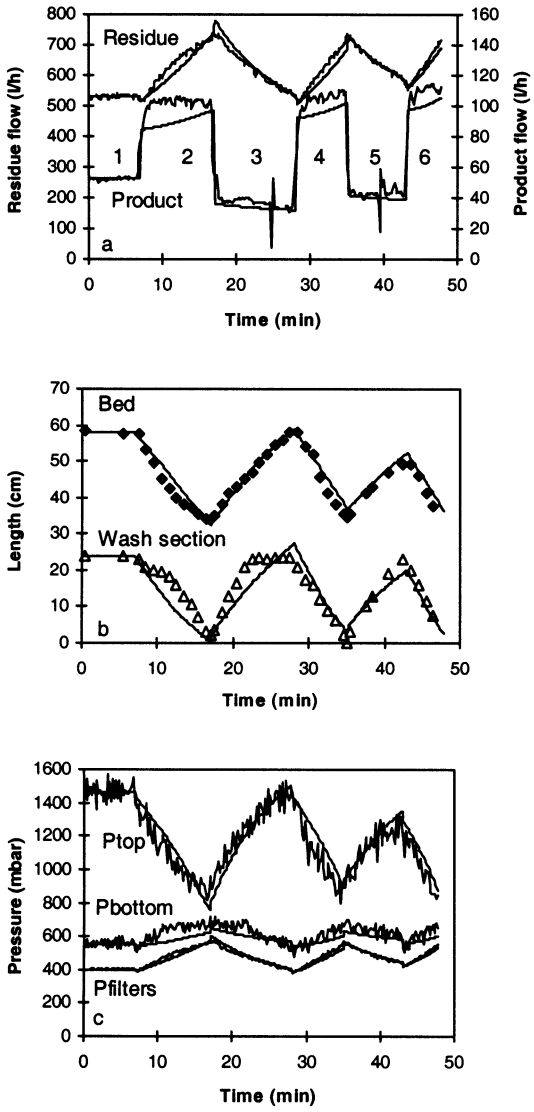

Figure 9. Changing the opening of the product valve.

(a) Product flow and residue flow; (b) length bed and wash section; (c) pressures.

The first point of interest is the time span needed to reach the new product flow. In the experiments, it takes about one minute before the largest part of the change in production is

Table 6. K_w Values

Period	K_w (Pa·s/m^3)
1	3.9×10^9
2	2.3×10^9
3	6.5×10^9
4	2.1×10^9
5	5.4×10^9
6	2.1×10^9

achieved, because it takes some time to carefully adjust the valve.

Both in the simulations and in the measurements the residue flow shows small jumps when the product valve is adjusted. Since the wash column contains a constant volume of material, an immediate change in one of the output flows directly results in an opposite change of another output flow. The fact that the simulated jumps in the residue flow are not always equal to the measured jumps is explained by a slip in the pump.

The sudden change in residue flow causes a sudden change in filter pressure, bottom pressure, and top pressure in the simulations. This is not detected in the validation experiments, because the simulated jumps are on the order of the scatter in the measured pressures. In forthcoming experiments it will be shown that for larger pressure changes these jumps were indeed detected in the wash column.

Predictions of the changes in the length of the crystal bed and the wash section between $t = 8$ and 18 min. and between $t = 18$ and 28 min are not fully satisfactory. The curvature of the predicted line is too straight in both cases. In addition, the predicted product flow is too small. The fact that the product valve was adjusted slightly several times between $t = 8$ and 18 min to keep a constant product flow explains the difference in production in this period. In period 3 to 6 no adjustments were made after the step and the deviations from the measured curves are smaller.

Validation in the pilot plant with storage vessel: Steering flow

In the pilot plant with the storage vessel, large step changes in the steering flow were applied to enforce pressure changes larger than the scatter caused by the pulsation of the feed pump. The main objective of the dynamic model is to predict the length of the bed and the wash section, but the pressure peaks also tell if the relation between flows and pressures is correctly defined in the model. Therefore, the steering flow was decreased by a large step from 726 L/h to 336 L/h at $t = 18$ min., and at $t = 52$ min it was increased from 336 L/h to 886 L/h. Figure 10a shows that the expected simulated pressure jump was indeed measured at the feed entrance. The effect of an abrupt pressure change in the top section is an abrupt change in the residue flow in both the simulation and the experiment.

However, even with these wide pressure changes no clear pressure jump in the bottom section was measured, although a small but abrupt jump was predicted. In addition, this predicted jump causes an abrupt change in the predicted product flow, which was not detected in the measurement. This indicates that the force balance in the dynamic model is probably simplifying the wash column behavior too much. The force balance causes the pressure jump in the bottom section whenever a large change in the top pressure occurs.

A final important point is the discrepancy between the predicted and measured Ptop, while the length of the bed is predicted reasonably well between 20 and 40 min. The supposition that this is caused by a change in the permeability of the bed appears to be confirmed by Figure 11b, which shows the increasing permeability of the top of the bed in time. However, it is debatable whether this is a real permeability change.

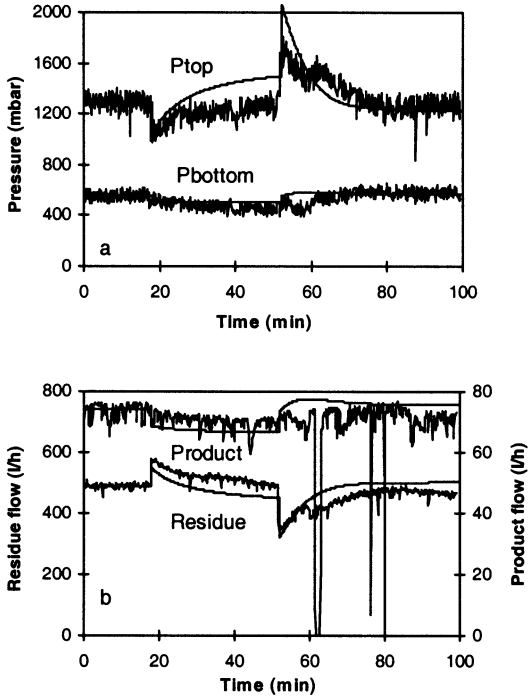

Figure 10. Pressures (a) and output flows (b) after step changes in the steering flow.

$t = 18$ min; φ_{steer} changes from 726 L/h to 336 L/h; $t = 52$ φ_{steer} changes from 336 L/h to 886 L/h.

The length of the bed increases very fast, but irregularly due to the large steps. At lengths above 65 cm the top of the bed tilted due to the hydrodynamics of the liquid. This obscures

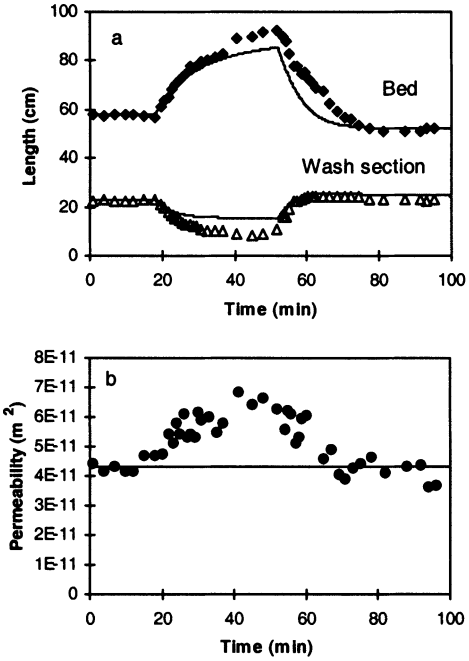

Figure 11. (a) Length of crystal bed and wash section after a step change in the steering flow; (b) permeability in the top section.

the validation experiment. Note that the increasing permeability cannot be due to consolidation, because that would result in a decreasing permeability between $t = 20$ and 40 min, as the top pressure was increasing during this period.

General discussion on model validation

The validation of the model in the previous section showed that it is now possible to predict trends in the dynamic behavior of the wash column and that basic phenomena, like coupling of pressures and flows, are described quite well. Still there are some theoretical and practical issues that should be addressed for further model improvement.

The value of the friction factor and the permeability determine the level of the bed and pressure levels in the new steady state. The assumptions of a constant friction factor in the wash column and a negligible compressibility of the bed are both questionable. Van Oord et al. (2002) showed that the bed is compacted in the top section, and the temperature change at the wash front will probably change the shape of the crystals. Both phenomena influence the friction with the wall. To incorporate this in the model, a method to measure the local friction factor has to be developed and axial porosity and permeability profiles have to be incorporated in the model.

For the simulations, quite a few of the parameters that are used in the simulation had to be derived from the measured steady-state values. To obtain a more detailed validation, more parameters should be measured directly, for example, the pressure drop over the valve and the crystal concentration. To predict wash-column behavior from first-principles information on the crystal and packed bed properties should be determined on-line and outside the wash column. In addition, the permeability in the bottom section is dependent on the permeability in the top section and the temperature change at the wash front, while the current model uses a separate parameter for the permeability above and below the wash front. More information on the phenomena taking place at the wash front is therefore needed.

Finally, it would be very interesting to validate the model for a nonmelt system, since such a system eliminates the heat balance so that less dependent variables play a role.

Control of a Hydraulic Wash Column

Design of a feedback control system

To use the hydraulic wash column on an industrial scale, automated control of the length of the crystal bed and the wash section is required. In the simulations of the model the steering flow appeared to be an appropriate control tool for the length of the bed, and the product valve was a control tool that influences both the length of the crystal bed and the length of the wash section. These observations are used to develop a feedback control system for the wash column. The dynamic model is used to examine the effectiveness of such a control system. The advantage of using the simulation program for the design of a control system is the possibility of taking nonlinear interactions into account. A disadvantage is that the model does not describe all phenomena in the wash column. The controller system should therefore always be tested in practice before implementation.

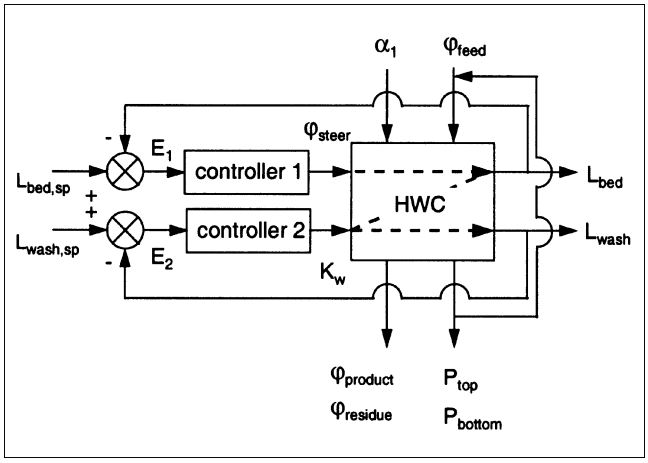

Figure 12. Feedback control scheme for the hydraulic wash column (HWC).

In a general feedback control system a sensor measures the value of the controlled output. For the position of the wash front the temperature can be used to detect the position, because of the temperature difference between the wash liquid and the feed slurry (Jansens et al., 1994a). For the position of the top of the bed, optical sensors seem the most suitable. The value of the measured output is compared with a given setpoint value, to give a deviation or error, E. The value of the error is transferred to a controller which changes the appropriate input variable. This often happens via a control element, like a valve (Stephanopoulos, 1984).

A feedback control system for the wash column is presented in Figure 12. The difference between the setpoint value of the bed length and the measured bed length results in a signal to controller 1, which causes a change in the steering flow. A deviation from the setpoint value for the position of the wash front activates controller 2, which changes the opening of the product valve so that K_w changes. When controller 2 is activated, both the length of the wash front and the length of the bed change, so that controller 1 will be activated again. The effects of a changed input variable, φ_{steer} or K_w, on the controlled outputs, L_{bed} and L_{wash}, is marked by the dotted lines in Figure 12.

To investigate the effectiveness of the designed control system for each controller, an equation was implemented in the dynamic model. A proportional integral (PI) controller was chosen, and the general description of it is given by Eq. 20. Here, $c(t)$ is the signal from the controller and consists of the bias controller signal, c_s, the error, $E(t)$, a controller gain, K_c , and an integral time constant, τ_c. The gain, K_c, determines how strong the controller acts on an error, while the integral time constant is the time needed by the controller to repeat the proportional action

$$c(t) = c_s + K_c \cdot E(t) + \frac{K_c}{\tau_c} \int_0^t E(t)\, dt \qquad (20)$$

In the dynamic model the calculated controller signal is defined as a percentage of the maximum value of the controlled variable. The error is the percentile deviation of the

set point, which results for the length of the wash section in the following equation

$$E(t) = \frac{(L_{\text{wash},sp} - L_{\text{wash}})}{L_{\text{wash},sp}} * 100 \qquad (21)$$

In the following sections first the controller settings are determined with the help of the dynamic model. Then the control system is tested for two types of control situations: a regulator problem, to keep the steady-state values when a disturbance in one of the inputs occurs, and a servo problem, in order to attain new setpoint values. Finally, the effect of the feedback control system on a range of disturbances is examined.

Determination of the controller settings

In principle many controller settings are possible; therefore, criteria for finding the optimal controller settings for the wash column have to be defined. The following criteria were used:

- In the steady state the length of the bed and the wash front may not deviate from the set point values. This means that proportional control alone is not sufficient, as this type of controller always has an off-set.
- The controller gain and time constant must be chosen such that the return to the set point occurs without too great a deviation from the set point value. For the bed an overshoot of 5 cm, and for the wash front an overshoot of 2 cm, is acceptable. For the wash front the overshoot is restricted because too low a wash front may allow the mother liquor to pollute the product, and this pollution is more likely when the wash front is not straight.
- The calculated values for the control variables K_w and φ_{steer} are restricted by the maximum capacity of the steering pump and the widest opening of the product valve.

For this multiple-input multiple-output system the controller settings were determined in the following way: in a simulation with both controllers active at $t = 10$ min (see Figure 13), the setpoint for the wash front or for the bed was changed. For the criteria given earlier, a proper control action should have a response time of less than 30 min, where the response time is defined as the time span between the step change and the moment after which the deviation from the desired setpoint no longer exceeds 5%. When this definition is used, several combinations of controller settings are possible. The controller settings summarized in Table 7 meet the preceding requirements without too many oscillations for setpoint changes of 5 cm in both the length of the wash section and the length of the bed.

Control after a disturbance: A regulator problem

The most probable disturbance in the inputs of the wash column is a change in the crystal fraction of the feed slurry, due to temperature or composition changes in the crystallizer. The closed-loop simulation for a 10% increase in the crystal fraction is shown in Figure 13 together with the open-loop response. Because of the scale of the graph, the bed length is represented by the length of the filtration section. With the control system the change in crystal fraction has no lasting effect on the length of the filtration and wash sections, while in an uncontrolled system, a higher bed level and a higher wash front would occur.

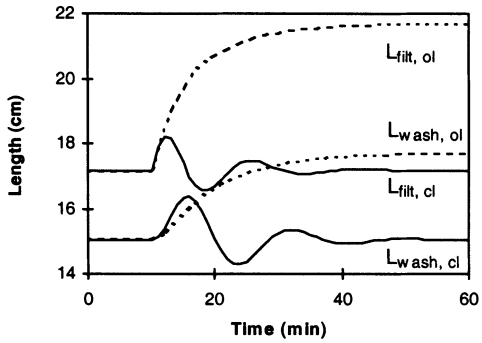

Figure 13. Length of the filtration section (L_{filt}) and length of the wash section (L_{wash}) after a step change of 10% in crystal fraction (0.114 to 0.125 v/v) of the feed slurry.

Open-loop (- -, ol) and closed-loop (—, cl) simulation.

Control to reach new setpoint values: A servo problem

The controller should track a new setpoint value for the level of the bed or for the position of the wash front in a reasonable time span, while it keeps the other level between the defined limits.

Figure 14 shows that with the controllers active it is possible to reach a new setpoint for the bed length. Note that once more the length of the filtration section (L_{filt}) is shown in this figure. The length of the bed is mainly controlled by the steering flow. The fluctuations in the length of the wash section in both Figure 14a and 14b are caused by the fact that the steering flow slightly influences the position of the wash front, which activates the second controller.

Figure 15 shows that according to the simulations, the controller is also able to direct the wash front to a new setpoint value. In the first instance, the length of the filtration section also changes, because the controller activates the valve, which has an effect both on the level of the wash front and on the level of the bed.

Limitations of the control system

To find the limits to the disturbances that the control system can cope with, the crystal fraction of the feed was changed in the simulations from its standard value of 0.114 to crystal fractions varying from 0.05 to 0.35. The controller is not able to keep the wash column between the defined safety limits when the crystal fraction is below 0.06 (v/v) or above 0.30 (v/v). With crystal fractions below 0.05, even the wash front disappears, which means pollution of the product. Crystal

Table 7. Controller Settings

Controller	c_s (%)	K_c	τ_c (s)
1 (φ_{steer})	27.8	−0.05	10
2 (K_w)	36.7	0.01	30

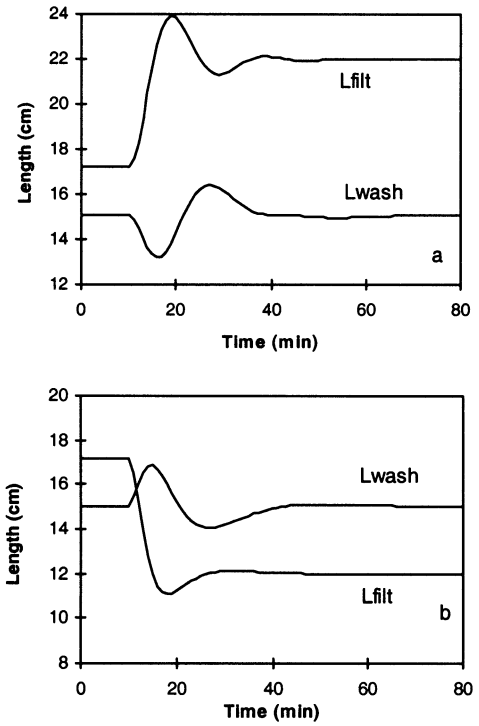

Figure 14. Simulated control action after a change in setpoint value for L_{filt} at $t = 10$ min; the setpoint for L_{wash} is kept at 15 cm.

Controller settings in Table 11. (a) $L_{filt,sp}$: 17.2 → 22 cm; (b) $L_{filt,sp}$: 17.2 → 12 cm.

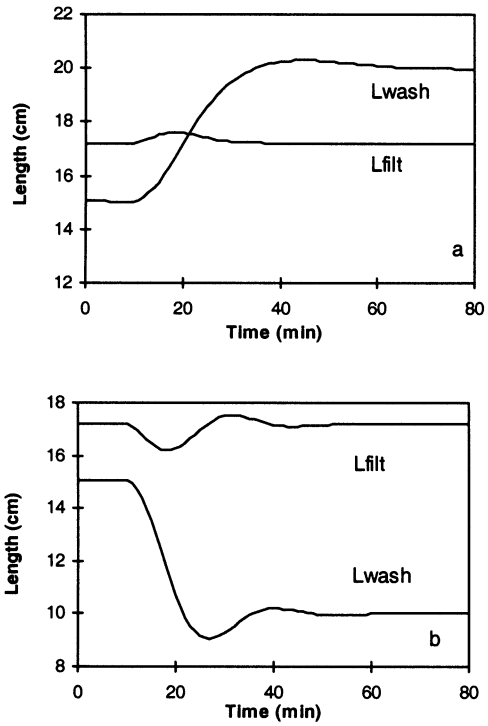

Figure 15. Simulated control action after a change in setpoint value for L_{wash} at $t = 10$ min; the setpoint for L_{filt} is kept at 17.2 cm.

Controller settings in Table 11. (a) $L_{wash,sp}$: 15 → 20 cm; (b) $L_{filt,sp}$: 15 → 10 cm.

fractions of the feed stream higher than 0.30 lead to a wash front that reaches the filters, which means loss of wash liquid. Table 8 summarizes the values of the overshoot for the length of the filtration and wash sections, together with the response time for the new crystal fraction. A response time of zero means that the deviation from the setpoint does not exceed 5%. It is shown that the acceptable margins for control (that is, 5 cm overshoot from the setpoint for the bed and 2 cm overshoot for the wash front) are only reached for small step changes of the crystal fraction. For a crystal fraction of 0.06, the defined setpoint for the bed cannot be reached, probably because the 17.2-cm setpoint value for the filtration section is just not possible under this feed condition, since a steady length of 12 cm is reached.

For crystal fractions higher than 0.125 (v/v), the overshoot for the wash front and the length of the bed again become too large; however, the controller is able to direct the levels to the desired set-point values. Operation of the wash column is thus still possible in these cases. It also has to be mentioned that in the simulations the crystal content of the feed was changed stepwise. In practice this is unlikely, since the temperature in the crystallizer, and, thus, the overshoots are likely to be lower and the crystal content of the feed will change gradually, which gives the controller more time to adjust.

Conclusions

A model was developed to simulate the dynamic behavior of a hydraulic wash column. The model combines slurry properties, wash-column dimensions, and input process conditions to predict the length of the crystal bed and the wash section, the pressure at the top and the bottom of the bed, and the product and residue flow rates.

The dynamic model was validated in a pilot plant with a pressure-dependent feed pump that was influenced by the pressure in the wash column. In the standard pilot plant containing a 70-L crystallizer and a 15.6-cm-diam wash column the validation experiments were obscured by the interaction between the crystallizer and the wash column. Integration of a storage vessel in the pilot plant diminished this interaction and facilitated larger steps in the input variables. The outputs were not predicted exactly, but the general trends in the length of the crystal bed and the wash-front height were fol-

Table 8. Overshoot (osh) and Response Time in Closed-Loop Simulation of the Model with a Step Change on the Crystal Fraction of the Feed

$\alpha_{1,new}$	Osh-Filt (cm)	Osh Wash (cm)	$t_{resp.}$ Filt (min)	$t_{resp.}$ Wash (min)
0.06	−13.25	−13.10	n.r.	110
0.10	−1.87	−3.26	0	19
0.125	+1.36	+1.98	0	27
0.15	+4.12	+5.26	6	21
0.20	+8.34	+9.11	6	22
0.25	+12.04	+10.98	7	23
0.30	+14.88	+12.06	14	23

n.r.: Setpoint not reached; $\alpha_{1,old} = 0.114$; $L_{filt,sp} = 17.2$ cm; $L_{wash,sp} = 15$ cm.

lowed satisfactorily. Further model improvement should primarily focus on the assumption of a constant friction factor and the compressibility of the bed.

Because the validation experiments showed that the simulations were representative of the wash-column behavior, the model was used to study the effect of control on the wash column. A feedback control system with two control loops was used to keep both the length of the bed and the wash front at desired setpoint values. Simulations with this extended model showed that the levels can easily be controlled for 10% step changes in the crystal content of the feed. Large overshoots occur when the crystal content increases more than 10%. However, no instability problems occur and the wash column can still be operated as long as the crystal fraction is between 0.06 and 0.30. When the set point for the length of the bed or the length of the wash front is changed, the control system is able to adjust the length of the wash section and the length of the bed to these changes.

Acknowledgment

The authors thank the NOVEM for financial support of the project. D. Verdoes and M. Nienoord from TNO-MEP are thanked for fruitful discussions and the use of the pilot plant. P. Huisjes and H. van der Meer are thanked for their skilled assistance during the experiments.

Notation

A_c = "open" cross-sectional area of the wash column, m^2
B = permeability, m^2
C = constant
$c(t)$ = controller signal, %
c_s = bias controller signal, %
C_l = solidification rate at the wash front (wash liquid), m^3/s
C_s = solidification rate at the wash front (solid), m^3/s
c_P = specific heat capacity, kJ/kg·K
D_c = diameter column, m
D_f = diameter filter tubes, m
D_h = hydraulic diameter of the column, m
E = deviation from setpoint, %
F_w = force due to friction, N
F_g = force due to gravity, N
ΔH_m = heat of fusion, kJ/kg
h = distance from top of bed, m
K = ratio between radial and axial stress
K_w = modified flow resistance factor, $Pa \cdot s/m^3$
K_f = friction factor
K_c = controller gain
$L_{filtration}$ = length of the filtration section, m
L_{wash} = length of the wash section, m
L_{bed} = total length of crystal bed, m
N = number of filter tubes, #
P_l = liquid pressure, Pa
ΔP_l = liquid pressure drop, Pa
P_{top} = liquid pressure above crystal bed, Pa
P_{bottom} = liquid pressure in melting circuit, Pa
T = temperature, K
V = volume, m^3
v_l = liquid velocity, m/s
v_s = solid velocity, m/s

Greek letters

α_1 = crystal fraction in the feed slurry, m^3/m^3
α_2 = crystal fraction in the slurry section, m^3/m^3
ϵ = porosity in the filtration and stagnant section
ϵ_w = porosity in the wash section
η_l = viscosity, Pa s
φ_{feed} = feed flow, m^3/s
$\varphi_{ml,\ filters}$ = mother liquor flow at the filters from top section, m^3/s
$\varphi_{ml,\ bottom}$ = mother liquor flow at the filters from bottom, m^3/s
$\varphi_{product}$ = product flow, m^3/s
$\varphi_{residue}$ = residue flow, m^3/s
$\varphi_{s,\ filters}$ = crystal flow at the filters, m^3/s
$\varphi_{s,\ knife}$ = crystal flow at the knife, m^3/s
φ_{steer} = steering flow, m^3/s
$\varphi_{wl,\ knife}$ = wash liquid flow at the knife, m^3/s
μ_w = wall friction coefficient
ρ_l = density of the liquid, kg/m^3
ρ_s = density of the solid, kg/m^3
σ = compressive stress, Pa
τ_c = controller integral time constant, s
τ_w = shear stress at the wall, Pa

Subscripts

cr = crystals
top = top section
slurry = slurry section
filtration = filtration section
wash = wash section
stagnant = stagnant zone
filters = at the filters

Literature Cited

Arkenbout, G. J. *Melt Crystallization Technology*, Technomic, Lancaster (1995).
Barton, P. I., and C. C. Pantelides, "Modeling of Combined Discrete/Continuous Processes," *AIChE J.*, **40**, 966 (1994).
Jansen, H. A., *2 Ver. Dtsch.*, Ing 3g, 1045 (1895).
Jansens, P. J, O. S. L. Bruinsma, G. M. van Rosmalen, and R. de Goede, "A General Control Strategy for Hydraulic Packed Bed Wash Columns," *Trans. Inst. Chem. Eng.*, **72A**, 695 (1994a).
Jansens, P. J, O. S. L Bruinsma, and G. M. van Rosmalen, "Compressive Stresses and Transport Forces in Hydraulic Packed Bed Wash Columns," *Chem. Eng. Sci.*, **49**, 3535 (1994b).
Nienoord, M, G. J. Arkenbout, and D. Verdoes, "Experiences with the TNO-Thijssen Wash Column," *Proc. Bremen Int. Workshop for Industrial Crystallization*, J. Ulrich, ed., Bremen, p. 4 (1994).
Schneiders, L. H. J. M., and G. J. Arkenbout, "Developing a High Efficiency Wash Column," *Filt. Sep.*, 304 (1986).
Shirato, M., M. Sambuichi, H. Kato, and T. Aragaki, "Internal Flow Mechanism in Filter Cakes," *AIChE J.*, **15**, 405 (1969)
Stephanopoulos, G. *Chemical Process Control: An Introduction to Theory and Practice*, Prentice-Hall, NJ (1984).
van Oord-Knol, L., *Hydraulic Wash Columns. Solid-Liquid Separation in Melt Crystallization*, PhD Thesis, Delft Univ. of Technology, Delft, The Netherlands (2000).
van Oord-Knol, L., O. S. L. Bruinsma, and P. J. Jansens, "Effect of Compressibility on the Performance of Hydraulic Wash Columns," *AIChE J.*, **48**(7), 1478 (2002).

Appendix

This appendix contains equations for calculating the compressive stress profile in each section of the wash column for incompressible beds.

Filtration section

$$\sigma_{\text{filtration}}(h) = \frac{A}{F} \cdot (e^{-F \cdot h} - 1) \tag{A1}$$

with

$$A = \frac{\Delta P_{l,\ \text{filtration}}}{L_{\text{filtration}}} = \frac{-\epsilon \cdot \eta}{B_{\text{filtration}}} \cdot \left(\frac{\varphi_{ml,\ \text{filters}}}{\epsilon \cdot A_c} - \frac{\varphi_{s,\ \text{filters}}}{(1-\epsilon) \cdot A_c} \right) \tag{A2}$$

$$F = \frac{4 \cdot K_f}{D_h} \tag{A3}$$

Stagnant zone

$$\sigma_{\text{stagnant}}\ (\text{filters}) = \sigma_{\text{filtration}}\ (\text{filters})$$

$$\sigma_{\text{stagnant}}(h) = -\frac{B}{F} + \frac{A}{F} \cdot e^{-F \cdot h} - \frac{A - B}{F} \cdot e^{(4K_f/D_h) \cdot (h - Lf)} \tag{A4}$$

where

$$B = \frac{\Delta P_{l,\,\text{stagnant}}}{L_{\text{stagnant}}} = \frac{-\epsilon \cdot \eta}{B_{\text{stagnant}}} \cdot \left(-\frac{\varphi_{ml\ \text{bottom}}}{\epsilon \cdot A_c} - \frac{\varphi_{s,\,\text{filters}}}{(1-\epsilon) \cdot A_c} \right) \tag{A5}$$

Lf = Length of the filtration section.

Wash section

$$\sigma_{\text{wash}}\ (\text{wash front}) = \sigma_{\text{stagnant}}\ (\text{wash front})$$

$$\sigma_{\text{wash}}(h) = -\frac{C}{F} + \frac{A}{F} \cdot e^{-F \cdot h} - \frac{A - B}{F} \cdot e^{-F \cdot (h - Lf)} + \frac{C - B}{F} e^{-F \cdot (h - Lf - Lst)} \tag{A6}$$

with

$$C = \frac{\Delta P_{l,\,\text{wash}}}{L_{\text{wash}}} = \frac{-\epsilon_w \cdot \eta}{B_{\text{wash}}} \cdot \left(-\frac{\varphi_{wl,\,\text{knife}}}{\epsilon_w \cdot A_c} - \frac{\varphi_{s,\,\text{knife}}}{(1-\epsilon_w) \cdot A_c} \right) \tag{A7}$$

Lst = Length of the stagnant zone.

Manuscript received July 13, 2001, and revision received Feb. 4, 2002.